ACS Macro Letters

Letter

pubs.acs.org/macroletters

Multidimensional Assembly of S-Layer Proteins on Mobility-Controlled Polyelectrolyte Multilayers

Seon Ju Yeo,[†,‡] Seong-Ho Shin,[†,§] Ki Tae Nam,*[,∥] and Pil J. Yoo*[,‡,⊥]

[‡]School of Chemical Engineering and [⊥]SKKU Advanced Institute of Nanotechnology (SAINT), Sungkyunkwan University, Suwon 440-746, Republic of Korea

[§]Molecular Foundry and Materials Sciences Division, Lawrence Berkeley National Laboratory, Berkeley, California 94720, United States

[∥]Department of Materials Science and Engineering, Seoul National University, Seoul 151-744, Republic of Korea

ABSTRACT: Polyelectrolyte multilayers have been vastly utilized as an assembling platform for various biomaterials because of their soft and charged surface characteristics, analogous to biomembrane systems. In particular, polyelectrolyte chains with high self-diffusivity can effectively transfer the surface mobility to the assembling biomolecular species, facilitating the ordered self-assembly. Herein, highly diffusional cationic polyelectrolyte chains of linear polyethylenimine are employed to induce direct binding with negatively charged bacterial surface layer proteins, which eventually lead to large-scale two-dimensional crystals. Notably, at the elevated incubation temperature, a transitory intermediate of one-dimensional chain structure is observed. We reveal that this one-dimensional intermediate is a stable precursor toward two-dimensional crystal arrays.

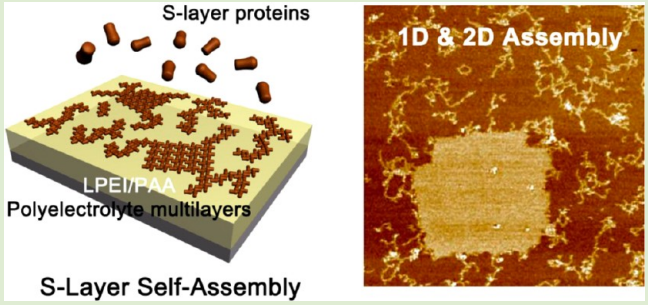

Bacterial surface layers (S-layers) form a compact crystalline array as the outermost cell envelope of many variant bacteria.[1,2] These crystalline arrays present various lattice symmetries carrying nanoscaled periodicities. Purified S-layer monomers assemble into two-dimensional crystals in the presence of metal ions and their lattices present the same periodicity and symmetry as the natural counterpart exhibits. This self-assembly holds promise for use in many applications such as providing a template for the formation of nanoparticles[3,4] or nanowire[5] arrays and the creation of patterning.[6,7] In particular, self-assemblies of S-layers on surfaces manifest their subtle impact on the assembly processes, while exhibiting multiple folding pathways and resultant morphologies.[8,9]

It has been implicated that bacterial membranes have a strong effect on the in vivo S-layer assembly and the interactions occurring between S-layer proteins and underlying membrane are directed by specific chemistry.[1,10,11] Therefore, revealing this process will enrich our basic understandings of S-layer assembly and, thus, expand the scope of S-layer engineering. However, the intrinsic heterogeneities and complexities of the bacterial membrane have made it difficult to discover its detailed roles and consequently, a reconstituted substrate is necessary to create a well-controlled system for investigating the S-layer assembly.[12] Similar to biological membranes, lipid bilayers provide a simple system with a well-characterized surface chemistry and physics.[8] Also, polyelectrolyte multilayer (PEM) films have been utilized for the S-layer assembly because they allow for charge-selective ordering characteristic of S-layers.[13−16]

Here we introduced a weakly charged PEM pair consisting of cationic linear polyethylenimine (LPEI) and anionic poly(acrylic acid) (PAA) in the S-layer assembly. In LPEI/PAA PEM film, the LPEI species becomes interdiffusional in the proper pH range due to the highly hydrated and hydrophilic nature of the LPEI backbone.[17,18] This interdiffusional behavior of LPEI can be optimally adjusted under conditions where the surface charge density is balanced with counterionic PAA.[19−22] In many assembly systems, the interdiffusion of LPEI imparts an ideal condition of strong surface mobility and minimized surface roughness (RMS roughness less than 1 nm) for the self-assembly while retaining the stable electrostatic binding between polyelectrolyte chains, which can eventually allow for a large-scale self-assembly of molecules that adsorb on the outermost surface of PEM. We envision that the lateral surface mobility of PEM can be harnessed directly to the self-assembly of S-layers.

Toward this goal, we focused on the surface mobility of PEM films as a key factor to determine the ordering characteristics of S-layers. We prepared LPEI/PAA PEM films at different pHs; in this way, the different level of charge density of LPEI develops accordingly, adjusting the interdiffusional behavior of LPEI. By modulating the lateral surface mobility of LPEI/PAA PEM films, we demonstrate that the self-assembly of S-layer proteins on the PEM films can be readily controlled with

Received: August 30, 2012
Accepted: October 5, 2012
Published: October 10, 2012

scalability, leading to crystalline two-dimensional (2D) structures over a large scale. The surface mobility becomes maximized further at elevated temperature. As a result, we observed, for the first time, the emergence of a one-dimensional (1D) precursor prior to its subsequent growth into the 2D lattice array. This unforeseen track can be attributed to the preferential and directional growth of S-layers upon being exposed to high surface mobility, which is only allowed at elevated temperatures.

Figure 1 shows a schematic of the different phases of S-layer assembly on LPEI/PAA PEM surface with varying surface

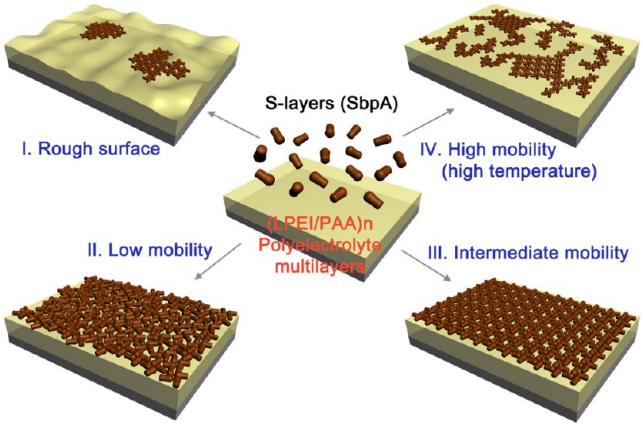

Figure 1. Schematic of different types of S-layer self-assembly on PEM films with varying surface mobilities.

mobilities. Purified from *Lysinibacillus sphaericus* (ATCC 4525, MW = 132 kDa), the monomeric S-layer protein (SbpA) was diluted in deionized water to the final concentration of 15 μg/mL with 1 mM $CaCl_2$; this divalent ion is required to initiate the assembly process on the surface. The pH of the protein solution was always adjusted to 5.2, which is above the isoelectric point (pH = 4.2) of SbpA.[23] In most cases, LPEI, a positively charged polyelectrolyte, lies on the outermost surface of a PEM film. The S-layer proteins with the opposite surface charge can be adsorbed directly by the electrostatic attractive interactions.

First, we investigated the effect of PEM surface conditions on the self-assembly behaviors of SbpA. It was previously determined that the relatively thick LPEI/PAA multilayer films deposited at pH 4.7−5.0 exhibit the highest surface mobility.[17,18] Therefore, as shown in Figure 2A, upon applying this condition for the S-layer self-assembly at ambient temperature, SbpA spontaneously crystallized to form highly ordered patches on LPEI/PAA films due to their enhanced surface mobility. Notably, the self-assembled structures were developed to large-scaled patches of ∼8 μm diameter in size without any noticeable defects. The canonical lattice structure of the SbpA crystal was confirmed in Figure 2B. Figure 2C shows a cross-sectional analysis of the S-layer assembled structure, which appeared as a monolayer with a height of around 8 nm.[24] By contrast, in other studies, the thickness of the S-layer crystallized on PEM surface was observed to be about 15 nm, implying the formation of bilayers.[13−15]

In comparison to previous results, where S-layer assemblies have been mainly conducted on a negatively charged top surface of PEM, the notable advantage of the current method is that the SbpA assembly in a large area can readily be obtained on the positively charged surface of LPEI. As demonstrated in

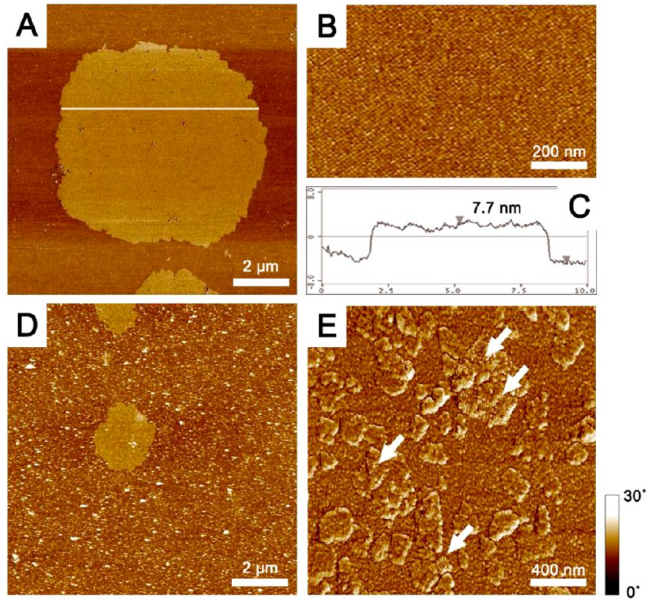

Figure 2. Phase-mode atomic force microscopic (AFM, Z-range = 30°) observation for different types of S-layer assembly at room temperature with varying the surface condition of PEM films. The nomenclature $(LPEI/PAA\ m/n)_x$ is used to indicate a multilayer film of LPEI/PAA pairs (x bilayer) deposited at pH m and n, respectively. When x includes 0.5, LPEI is the final adsorbed layer and thus the outermost surface of the multilayer. (A) Large-area two-dimensional assembly of S-layers on $(LPEI/PAA\ 4.7/4.7)_{9.5}$. (LPEI top, scan size = 10 × 10 μm^2). (B) Magnified images of (A) exhibiting apparent square lattice symmetry (p4) of S-layers (scan size = 1 × 0.6 μm^2). (C) Cross-sectional analysis for white line in (A). (D) Small-area assembly of S-layers on $(LPEI/PAA\ 4.7/4.7)_{3.0}$ (PAA top, scan size = 10 × 10 μm^2). Fewer bilayer numbers of 3.0 is employed for avoiding the surface roughening of PAA-treated films with greater bilayer numbers. (E) Localized array patches (marked as white arrows) of loosely assembled S-layers on $(PAH/PAA\ 7.5/3.5)_{3.5}$ (scan size = 2 × 2 μm^2).

Figure 2D, although the crystals of SbpA were observed on the negatively charged PAA surface, their morphologies were quite different and the assembled size was small. To verify the role that the surface mobility of LPEI plays in S-layer self-assembly, we compared the crystallization process of S-layer proteins on other types of a positively charged polyelectrolytes without self-diffusivity. When the SbpA monomers were assembled on poly(allylamine hydrochloride) (PAH)-treated surface of $(PAH/PAA\ 7.5/3.5)_{3.5}$ multilayers, the localized array patches of S-layers without long-range order only formed as shown in Figure 2E. Randomly formed patches of nonspecifically bound S-layers are attributed to unfavorable surface properties of PAH for the self-assembly, such as a lack in mobility, increased surface roughness (RMS roughness ∼ 2.5 nm) and greater hydrophobicity due to the higher pK_a of primary amines.[13,14]

Next, we compared S-layer self-assembly on PEM surfaces with the different mobilities. As has been verified from previous work on viral self-assembly, the interdiffusion capability and the surface mobility of LPEI species can be manipulated primarily by adjusting the preparation pH of PEM films because the degree of ionization of LPEI and its chain conformation are accordingly varied.[18] Therefore, the pH of each layer in a PEM film ranges between 3.0 and 4.7, under which the surface mobility of LPEI is dramatically changed, from almost frozen at pH 3.0 to highly mobile at pH 4.7. Combined with this pH variation, we employed an additional variable of incubation

dx.doi.org/10.1021/mz3004538 | *ACS Macro Lett.* 2012, 1, 1254−1257

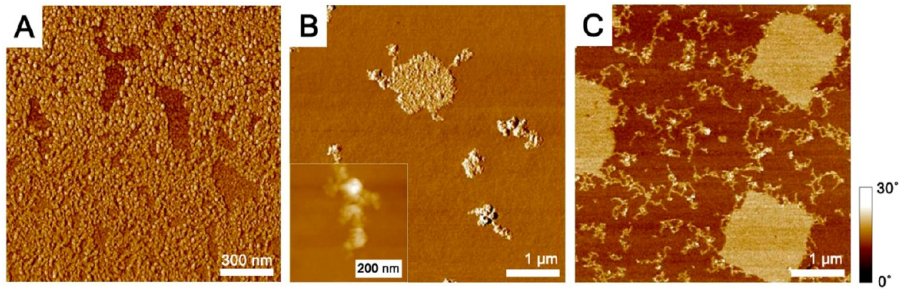

Figure 3. Effect of PEM deposition pH on the structures of S-layer self-assembly under an elevated temperature at 50 °C. Phase mode AFM images captured under ambient temperature (Z-range = 30°). (A) Random adsorption of S-layer proteins on $(LPEI/PAA\ 3.0/3.0)_{12.5}$. (scan size = 1.5 × 1.5 μm^2) (B) Relatively small-area 2D and short-chained 1D assemblies of S-layers on $(LPEI/PAA\ 4.0/4.0)_{10.5}$ (scan size = 5 × 5 μm^2). Inset shows a magnified height-mode AFM image of the irregularly stacked agglomeration of S-layers. (scan size = 500 × 500 nm^2, Z-range = 100 nm) (C) Coexistence of large-area 2D and chained 1D assemblies on $(LPEI/PAA\ 4.7/4.7)_{9.5}$ (scan size = 5 × 5 μm^2).

temperature for the S-layer self-assembly. The lateral diffusion of adsorbed S-layer monomers was tuned to their association at the elevated temperature, which can consequently result in different assembly behaviors compared to those under ambient conditions.

Previous research has revealed that the SbpA crystal on the negatively charged polyelectrolyte surface, such as poly(styrene sulfonate) (PSS),[15] loses its crystallinity at 55 °C, whereas the one on the secondary cell wall polymer maintains its lattice up to 70 °C.[25] However, neither cases provided any information on the thermostability of intermediates during the SbpA assembly. Although we found these S-layer crystals on the positively charged LPEI surface retain their crystallinity up to 60 °C, the incubation was performed at 50 °C to avoid the denaturation of SbpA monomers and intermediates toward the SbpA crystal state.[26] After the incubation for a given period of time, the samples were immediately quenched to ambient temperature and examined with AFM.

The influences of the surface mobility on the S-layer self-assembly are presented in Figure 3. In each case, the S-layer solution at pH 5.2 was applied to 120 nm thickness films of LPEI/PAA PEM at 50 °C. On the LPEI-treated surface of $(LPEI/PAA\ 3.0/3.0)_{12.5}$, a number of S-layers were adsorbed and arrested on the surface (Figure 3A). This observation indicates that the assembly of the adsorbed proteins does not proceed further due to either the increased charge density of LPEI or the absence of the surface mobility. On the other hand, in the case of two different PEM films, $(LPEI/PAA\ 4.0/4.0)_{10.5}$ and $(LPEI/PAA\ 4.7/4.7)_{9.5}$, 1D structures of filaments were observed as shown in Figure 3B,C. For the case of $(LPEI/PAA\ 4.0/4.0)_{10.5}$ relatively short length 1D chains and small 2D assembled domains lacking order were formed. The thickness of these structures, especially for 1D chains, varied from 5 to 30 nm. As revealed in the inset of Figure 3B, a short length 1D structure seemed to be a random agglomerate of S-layer monomers. In comparison, for the case of $(LPEI/PAA\ 4.7/4.7)_{9.5}$, 1D structures of hair-like chains were elongated with a diameter of 4−5 nm. Simultaneously, large 2D crystalline patches with exhibiting a constant height (∼8 nm) were observed, corresponding to the monolayer crystal (Figure 3C). This apparent difference in the assembly morphologies depending on PEM deposition pH is primarily attributed to the degree of the surface mobility on the PEM films.

Notably, an important question arises here as to how the S-layer monomers can be transformed into 1D and 2D assembled structures concurrently. It has been recently reported that S-layer assembly from the monomer to the ordered crystal can undergo multiple kinetic pathways.[9] In our case, the S-layer self-assembly at room temperature leads to the final crystal state without the 1D structure to reach the energetically favored 2D crystalline array. However, for the case of assembly under an elevated temperature, it can be reasoned that the 1D structure emerges as an additional intermediate and its transformation into the 2D crystal is subsequent to the associated condensation, which is not allowed for the assembly at ambient condition. Therefore, the 1D filament structure of S-layers is a transitory phase toward the formation of a 2D crystalline array; this phase exists only under the condition of enhanced surface mobility.

To confirm that the 1D chain structure is an intermediate toward the 2D crystal, the adsorption of SbpA monomers and their assembly process at elevated temperature were investigated ex situ (Figure 4). The overall process is reminiscent of

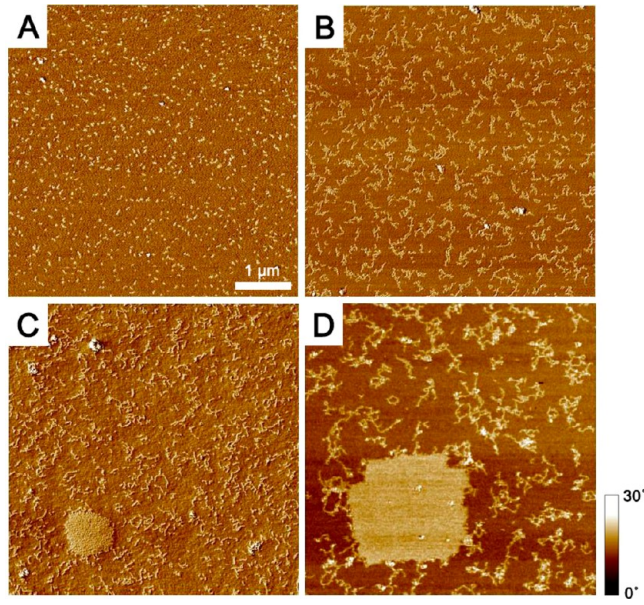

Figure 4. Progressive growth of S-layer self-assembly from 1D filaments to crystallized 2D patches under an elevated temperature of 50 °C (phase mode AFM images captured under ambient temperature, scan size = 5 × 5 μm^2, Z-range = 30°). (A) After 30 min, S-layer monomers were adsorbed. (B) After 2 h, S-layer monomers gradually grew to 1D chain structures. (C) After 5 h, noncrystalline small-sized 2D patches formed. (D) After 12 h, monolayered 2D patches were crystallized and grew larger with square lattice array (p4).

dx.doi.org/10.1021/mz3004538 | *ACS Macro Lett.* 2012, 1, 1254−1257

the multistep pathway of SbpA assembly on lipid bilayers: adsorbed proteins, an amorphous intermediate and its transition to the tetramer lattice crystal.[8,9] Similarly, S-layer monomers with a thickness of about 1−2 nm are randomly adsorbed atop the LPEI surface (Figure 4A). The adsorbed proteins develop 1D chain structures preferentially with a thickness of 4−5 nm during the following 2 h (Figure 4B). As time further elapses (5 h), the adjacently grouped 1D chains begin to assemble and form amorphous clusters. Their thickness, 9−10 nm, is a little bit larger than that of the crystalline monolayer (Figure 4C). Finally, 2D crystals with a thickness of about 7−8 nm are formed on the surface (Figure 4D). The slightly reduced thickness of the crystal implies that the structural rearrangement takes place during the transition to the completely crystallized phase. Indeed, it should be noted that the crystalline phase subsequently emerges from the amorphous clusters on the surface rather than from the crystals preformed in solution. Also, the crystal boundaries captured in Figure 4D clearly show that 1D chains are consumed and gradually grown into a 2D array structure. This observation explains how the S-layer protein can assemble into an intermediate 1D filament structure on the highly diffusive surface at the elevated temperature.

In summary, we have studied S-layer self-assembly on mobility-modulated polyelectrolyte multilayer films by employing self-diffusional polyelectrolyte chains of LPEI. This tunability of the surface mobility exhibits a synergistic effect on the S-layer assembly process at an elevated temperature. On the optimized surface of the highly mobile PEM, the S-layer assembly tracks a multistep pathway where the emergence of the 1D structures and their condensation by themselves occur prior to the crystal transformation. Although it is still preliminary to generalize the S-layer crystallization in an in vivo biological situation, our study suggests that the mobility control of proteins can provide an additional route to determine the assembly behavior.

AUTHOR INFORMATION

Corresponding Author

*E-mail: nkitae@snu.ac.kr; pjyoo@skku.edu.

Author Contributions

†These authors contributed equally to this work

Notes

The authors declare no competing financial interest.

ACKNOWLEDGMENTS

This work was supported by Basic Science Research Program grants (2010-0009877, 2010-0029409, 2012-0004117) and research grant (NRF-C1AAA001-2010-0028962) through the National Research Foundation of Korea (NRF) funded by the Korea Government (MEST). K.T.N. appreciates support by the Global Frontier R&D Program on Center for Multiscale Energy System (2011-0031574).

REFERENCES

(1) Sleytr, U. B.; Messner, P.; Pum, D.; Sara, M. *Angew. Chem., Int. Ed.* **1999**, *38*, 1035−1054.
(2) Pavkov-Keller, T.; Howorka, S.; Keller, W. *Prog. Mol. Biol. Transl. Sci.* **2011**, *103*, 73−130.
(3) Shenton, W.; Pum, D.; Sleytr, U. B.; Mann, S. *Nature* **1997**, *389*, 585−587.
(4) Mark, S. S.; Bergkvist, M.; Yang, X.; Teixeira, L. M.; Bhatnagar, P.; Angert, E. R.; Batt, C. A. *Langmuir* **2006**, *22*, 3763−3774.
(5) Sierra-Sastre, Y.; Choi, S.; Picraux, S. T.; Batt, C. A. *J. Am. Chem. Soc.* **2008**, *130*, 10488−10489.
(6) Gyorvary, E. S.; O'Riordan, A.; Quinn, A. J.; Redmond, G.; Pum, D.; Sleytr, U. B. *Nano Lett.* **2003**, *3*, 315−319.
(7) Liu, J. R.; Mao, Y. B.; Lan, E.; Banatao, D. R.; Forse, G. J.; Lu, J.; Blom, H. O.; Yeates, T. O.; Dunn, B.; Chang, J. P. *J. Am. Chem. Soc.* **2008**, *130*, 16908−16913.
(8) Chung, S.; Shin, S.-H.; Bertozzi, C. R.; De Yoreo, J. J. *Proc. Natl. Acad. Sci. U.S.A.* **2010**, *107*, 16536−16541.
(9) Shin, S.-H.; Chung, S.; Sanii, B.; Comolli, L. R.; Bertozzi, C. R.; De Yoreo, J. J. *Proc. Natl. Acad. Sci. U.S.A.* **2012**, *109*, 12968−12973.
(10) Sleytr, U. B.; Huber, C.; Ilk, N.; Pum, D.; Schuster, B.; Egelseer, E. M. *FEMS Microbiol. Lett.* **2007**, *267*, 131−144.
(11) Albers, S. V.; Meyer, B. H. *Nat. Rev. Microbiol.* **2011**, *9*, 414−426.
(12) Moreno-Flores, S.; Kasry, A.; Butt, H. J.; Vavilala, C.; Schmittel, M.; Pum, D.; Sleytr, U. B.; Toca-Herrera, J. L. *Angew. Chem., Int. Ed.* **2008**, *47*, 4707−4710.
(13) Toca-Herrera, J. L.; Krastev, R.; Bosio, V.; Kupcu, S.; Pum, D.; Fery, A.; Sara, M.; Sleytr, U. B. *Small* **2005**, *1*, 339−348.
(14) Delcea, M.; Krastev, R.; Gutlebert, T.; Pum, D.; Sleytr, U. B.; Toca-Herrera, J. L. *J. Nanosci. Nanotechnol.* **2007**, *7*, 4260−4266.
(15) Delcea, M.; Krastev, R.; Gutberlet, T.; Pum, D.; Sleytr, U. B.; Toca-Herrera, J. L. *Soft Matter* **2008**, *4*, 1414−1421.
(16) Dronov, R.; Kurth, D. G.; Mohwald, H.; Scheller, F. W.; Friedmann, J.; Pum, D.; Sleytr, U. B.; Lisdat, F. *Langmuir* **2008**, *24*, 8779−8784.
(17) Yoo, P. J.; Nam, K. T.; Qi, J. F.; Lee, S. K.; Park, J.; Belcher, A. M.; Hammond, P. T. *Nat. Mater.* **2006**, *5*, 234−240.
(18) Yoo, P. J.; Zacharia, N. S.; Doh, J.; Nam, K. T.; Belcher, A. M.; Hammond, P. T. *ACS Nano* **2008**, *2*, 561−571.
(19) Picart, C.; Mutterer, J.; Richert, L.; Luo, Y.; Prestwich, G. D.; Schaaf, P.; Voegel, J. C.; Lavalle, P. *Proc. Natl. Acad. Sci. U.S.A.* **2002**, *99*, 12531−12535.
(20) Lavalle, P.; Vivet, V.; Jessel, N.; Decher, G.; Voegel, J. C.; Mesini, P. J.; Schaaf, P. *Macromolecules* **2004**, *37*, 1159−1162.
(21) Zacharia, N. S.; DeLongchamp, D. M.; Modestino, M.; Hammond, P. T. *Macromolecules* **2007**, *40*, 1598−1603.
(22) Zacharia, N. S.; Modestino, M.; Hammond, P. T. *Macromolecules* **2007**, *40*, 9523−9528.
(23) Sara, M.; Sleytr, U. B. *J. Bacteriol.* **2000**, *182*, 859−868.
(24) Gyorvary, E. S.; Stein, O.; Pum, D.; Sleytr, U. B. *J. Microsc. (Oxford, U.K.)* **2003**, *212*, 300−306.
(25) Toca-Herrera, J. L.; Moreno-Flores, S.; Friedmann, J.; Pum, D.; Sleytr, U. B. *Microsc. Res. Tech.* **2004**, *65*, 226−234.
(26) Teixeira, L. M.; Strickland, A.; Mark, S. S.; Bergkvist, M.; Sierra-Sastre, Y.; Batt, C. A. *Macromol. Biosci.* **2010**, *10*, 147−155.